Impedance Spectroscopy of Petroleum Fluids at Low Frequency

Lamia Goual*

Department of Chemical and Petroleum Engineering, University of Wyoming, 1000 East University Avenue, Laramie, Wyoming 82071

Received October 7, 2008. Revised Manuscript Received January 19, 2009

Impedance spectroscopy enables fast and nondestructive dielectric characterization of petroleum fluids during different stages of exploration and processing. The majority of existing studies focused on frequencies above 10^3 Hz. The advantage of considering smaller frequencies is that more information on the electrical conductivity of the sample can be extracted. In this work, dielectric relaxation measurements on Boscan asphaltenes and maltenes are performed by impedance spectroscopy in the low-frequency range of $40-10^6$ Hz. The data are analyzed within the formalism of complex impedance. As frequency increases, the system shifts from highly conducting below ~10 Hz to highly insulating above 10^5 Hz. A comparison of impedance with electric modulus and permittivity suggests that only one primary relaxation mechanism exists between 10 and 10^5 Hz because of conductance effects. The alternating-current (AC) conductivity is almost independent of frequency below 10^5 Hz and increases with increasing frequency above this range. Extrapolation of AC conductivity to zero frequency provides an estimate of direct-current (DC) conductivity, from which the molecular size of asphaltenes can be determined. In addition, the onset of asphaltene aggregation can be detected from the variations of DC conductivity with asphaltene concentration in toluene. Thus, low-frequency dielectric relaxation is a simple and powerful tool to predict asphaltene-associated problems in the field.

1. Introduction

Dielectric relaxation techniques have been widely employed to investigate relaxation processes in petroleum fluids and the dependence of their characteristics on asphaltene aggregation. Impedance spectroscopy is particularly attractive because it enables fast and nondestructive dielectric characterization of petroleum fluids during different stages of exploration and processing.[1,2] Dependent upon the frequency range, the complex electrical behavior of asphaltenes may result from their dipolar response, their conductive response, or both. The dipolar component is usually associated with the orientation of permanent dipoles[1,3,4] and can be described by the Cole−Cole formalism,[5] whereas the conductive component reflects the translation of charges among the π orbitals of polynuclear aromatics.[6,7]

Previous dielectric relaxation studies on various crude oils showed a dipolar relaxation in the megahertz region and a low-frequency conductivity.[1,2] The dipolar relaxation of asphaltenes in toluene depends upon their aggregation state. In addition to a dipolar relaxation observed in the megahertz region, Sheu and co-workers[8] recorded a second peak in the dielectric loss spectra of asphaltene aggregates at 10^5 Hz, possibly a result of caging effects in large clusters, which restricted their rotational dynamics. The same authors claimed that, in such systems, the measured dipoles are largely induced dipoles and that the electrical conductivity may originate from rapid charge exchange between asphaltene aggregates. This mechanism is also known as Maxwell−Wagner interfacial polarization.[9] Syunyaev et al.[3] reported the existence of three relaxation peaks in the dielectric loss spectra of pyrolysis tar in benzene using time-domain dielectric spectroscopy. The peaks were observed in the frequency range of $0.2-20 \times 10^6$ Hz (first band), $20-250 \times 10^6$ Hz (second band), and $250-2500 \times 10^6$ Hz (third band). The relaxation processes were attributed to dipole-orientation polarization and described by the Cole−Cole formalism. Using the same technique on a vacuum residue in toluene, Evdokimov and Eliseev[4] recorded two peaks in the dielectric loss spectra at 80×10^6 and 220×10^6 Hz, respectively. The first peak was related to the relaxation of large particles and complexes, while the second peak was due to the relaxation of macromolecular asphaltene and resin components.

Almost all previous dielectric relaxation studies were performed at frequencies above 10^3 Hz to avoid electrode polarization effects. However, these effects can be minimized with the advent of new technology and proper calibration procedures. To our best knowledge, no dielectric relaxation spectra of petroleum fluids are currently available below 10^3 Hz. The

* To whom correspondence should be addressed. Telephone: 307-766-3278. E-mail: lgoual@uwyo.edu.

(1) Tjomsland, T.; Hilland, J.; Christy, A. A.; Sjoblom, J.; Riis, M.; Friiso, T.; Folgero, K. Comparison of infrared and impedance spectra of petroleum fractions. *Fuel* **1996**, *75* (3), 322–332.

(2) Folgero, K. Broad-band dielectric spectroscopy of low-permittivity fluids using one measurement cell. *IEEE Trans. Instrum. Meas.* **1998**, *47* (4), 881–855.

(3) Syunyaev, R. Z.; Kaprov, S. A.; Kaprova, V. V. Study of the disperse structure of petroleum by time-domain dielectric spectroscopy. *Chem. Technol. Fuels Oils* **2001**, *37* (2), 131–133.

(4) Evdokimov, I. N.; Eliseev, N. Y. Electrophysical properties of liquid hydrocarbon media. *Chem. Technol. Fuels Oils* **2001**, *37* (1), 39–43.

(5) Cole, K. S.; Cole, R. H. Dispersion and absorption in dielectrics. *J. Appl. Phys.* **1941**, *9*, 341–351.

(6) Maruska, H. P.; Forster, E. O.; Enard, J. H. Electrical transport processes in heavy hydrocarbon fluids. *IEEE Trans. Dielectr. Electr. Insul.* **1985**, *20* (6), 947–955.

(7) Siffert, B.; Kuczinski, J.; Papirer, E. Relationship between electrical charge and flocculation of heavy oil distillation residues in organic medium. *J. Colloid Interface Sci.* **1990**, *135* (1), 107–117.

(8) Sheu, E. Y.; Storm, D. A.; Shields, M. B. Dielectric response of asphaltenes in solvent. *Energy Fuels* **1994**, *8*, 552–556.

(9) Maxwell, J. C. *A Treatise on Electricity and Magnetism*; Courier Dover Publications: New York, 1954; Vol. 1.

10.1021/ef800860x CCC: $40.75 © 2009 American Chemical Society
Published on Web 02/19/2009

advantage of considering small frequencies is that more information on the electrical conductivity of the sample can be extracted.

Early studies on the electrical conductivity of asphaltenes showed that asphaltene conductivity increases with increasing asphaltene concentration, temperature, and dielectric constant of solvent.[10] Maruska et al.[6] studied the conductivity of catalytic cracking residues in various aromatic and aliphatic solvents. They recorded a maximum in direct-current (DC) conductivity with solvent weight fraction because of competitive effects between ionic mobility and viscosity of the blend. Fotland and Anfindsen[11] used the theoretically based Fuoss model to describe the variations of DC conductivity with asphaltene concentration at very high aromatic solvent dilution. They found three regions separated by two breakpoints in the conductivity versus concentration curve. The first region corresponds to free ions and ion pairs; the second region corresponds to triple ions; and the third region corresponds to higher aggregates. More recently, Sheu and Mullins[12] found that alternating-current (AC) conductivity remains almost constant with a frequency up to a critical value of 5.6×10^5 Hz, above which a sudden increase in AC conductivity occurs because of a charge-transformation mechanism. In another study, Sheu et al.[13] found that AC conductivity normalized by asphaltene concentration decreases monotonically with asphaltene concentration and the discontinuity of this function was associated with the onset of asphaltene association.

This paper aims at investigating the dielectric relaxation of asphaltenes and maltenes at relatively low frequencies ($40-10^6$ Hz). At this frequency range, conduction effects are believed to play a key role. Thus, an important motivation of this work is to enhance our basic understanding of relaxation processes in petroleum fluids because of the presence of charge carriers. The combination of several dielectric functions, such as complex impedance, electric modulus, and permittivity, allows for a better interpretation of the processes involved. In particular, the differences between conduction and dipolar relaxation within the bulk of the fluid are discerned. The advantage of using impedance and modulus formalisms is that the modulus captures both conduction and dipolar relaxation processes, while impedance captures only dipolar relaxation. Moreover, the use of AC field reduces problems that might be encountered with electrode polarization effects. The results of Boscan asphaltenes and maltenes are presented in this paper. Asphaltenes and maltenes extracted from lighter crude oils gave similar trends.

2. Theory

The complex impedance, permittivity, and modulus are defined as

$$Z = Z' + jZ'' \tag{1}$$

$$\varepsilon = \frac{1}{j\omega C_0 Z} = \varepsilon' - j\varepsilon'' \tag{2}$$

$$M = \frac{1}{\varepsilon} = M' + jM'' \tag{3}$$

where $j = \sqrt{(-1)}$, Z', and Z'' are measured directly by the impedance analyzer. The real and imaginary parts of the other dielectric functions are calculated from

$$\varepsilon' = \frac{-Z''}{|Z|^2 \omega C_0} = \frac{C_p}{C_0} \tag{4}$$

$$\varepsilon'' = \frac{Z'}{|Z|^2 \omega C_0} = \frac{1}{\omega C_0 R_p} \tag{5}$$

$$M' = \frac{\varepsilon'}{\varepsilon'^2 + \varepsilon''^2} \tag{6}$$

$$M'' = \frac{\varepsilon''}{\varepsilon'^2 + \varepsilon''^2} \tag{7}$$

where $\omega = 2\pi f$ is the angular frequency, $C_0 = \varepsilon_0 A/t$ is the capacitance of free space, ε_0 is the permittivity of free space (8.854×10^{-12} F/m), A is the cross-sectional area of the electrodes (0.001 134 m^2), and t is the gap between electrodes (10^{-3} m). C_p and R_p are the capacitance and resistance of the electric circuit, respectively.

The absolute impedance, $|Z|$, and phase angle, θ, are then expressed by

$$|Z| = \sqrt{Z'^2 + Z''^2} \tag{8}$$

$$\tan\theta = \frac{Z''}{Z'} \tag{9}$$

Similarly, the absolute permittivity, $|\varepsilon|$, and loss tangent or dissipation factor, $\tan\delta$, are determined from

$$|\varepsilon| = \sqrt{\varepsilon'^2 + \varepsilon''^2} \tag{10}$$

$$\tan\delta = \frac{\varepsilon''}{\varepsilon'} = -\frac{Z'}{Z''} \tag{11}$$

The frequency dependence of the complex dielectric permittivity is often described by the Cole−Cole equation[5]

$$\varepsilon = \varepsilon_\infty + \frac{\varepsilon_s - \varepsilon_\infty}{1 + (j\omega\tau)^{1-\alpha}} - j\frac{\sigma_{DC}}{\omega\varepsilon_0} \tag{12}$$

where σ_{DC} is the DC conductivity, α represents the distribution of relaxation times, τ is the relaxation time ($\tau = C_p R_p$), and ε_s and ε_∞ are the permittivity of the solute (i.e., asphaltenes and maltenes) and solvent (i.e., toluene), respectively.

3. Experimental Section

3.1. Materials. Materials include toluene and heptane, both reagent grade from Fisher Scientific. The crude oil used in this work is from Boscan (Venezuela). This crude contains 18.8 wt % C_7 asphaltenes and about 36 wt % resins. C_7 asphaltenes are separated by mixing 1 g of crude oil to 40 vol of *n*-heptane. The mixture is left overnight and then filtered using a Whatman filter paper (47×10^{-3} m diameter and 0.2×10^{-6} m pore size). The precipitated asphaltenes are extensively washed with heptane, dissolved in toluene, and then dried after toluene evaporation. Maltenes are collected from the liquid filtrate after *n*-heptane evaporation. To quantify the amount of resins in the maltenes, resins are extracted according to a procedure presented elsewhere.[14]

3.2. Apparatus. Low-frequency impedance measurements are conducted using a 4294A precision impedance analyzer (Agilent, Santa Clara, CA) with a wide frequency range from 40 to 110×10^6 Hz. The impedance analyzer is connected to a 16452A liquid test fixture (Agilent, Santa Clara, CA) through a 16048G 1 m port extension cable with four terminals (Agilent, Santa Clara, CA). The

(10) Penzes, S.; Speight, J. G. Electrical conductivities of bitumen fractions in non-aqueous solvents. *Fuel* **1974**, *53*, 192–197.

(11) Fotland, P.; Anfindsen, H. Conductivity of asphaltenes. In *Structure and Dynamics of Asphaltenes*; Mullins, O. C., Sheu, E. Y., Eds.; Plenum: New York, 1998.

(12) Sheu, E. Y.; Mullins, O. C. Frequency-dependant conductivity of Utah crude oil asphaltene and deposit. *Energy Fuels* **2004**, *18*, 1531–1534.

(13) Sheu, E. Y.; Long, Y.; Hamza, H. Asphaltene self-association and precipitation in solvents—AC conductivity measurements. In *Asphaltenes, Heavy Oils, and Petroleomics*; Mullins, O. C., Sheu, E. Y., Hammami, A., Marshall, A. G., Eds.; Springer: New York, 2007.

(14) Goual, L.; Firoozabadi, A. Measuring asphaltenes and resins and dipole moment in petroleum fluids. *AIChE J.* **2002**, *48* (11), 2646–2663.

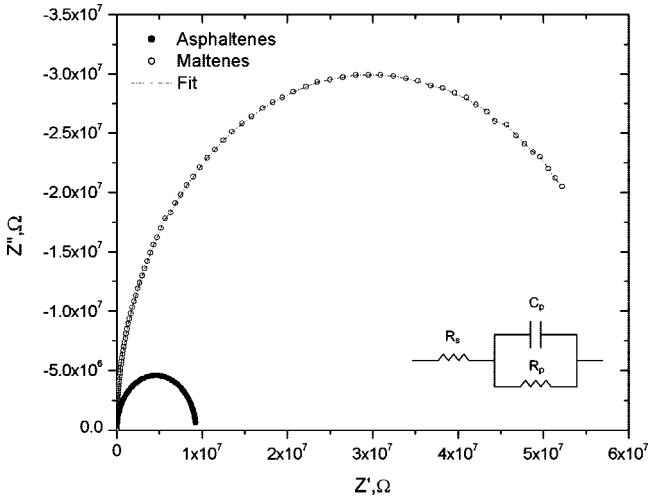

Figure 1. Nyquist plot of 0.824×10^{-3} kg/L asphaltenes and 3.617×10^{-3} kg/L maltenes in toluene.

operating frequency of the test fixture is from 20 to 30×10^6 Hz. The cell has a volume capacity of 4.8×10^{-3} L and comports two nickel-coated cobalt electrodes with 10^{-3} m spacing between them. A total of 40 point average measurements are performed under frequency sweep from 40 to 10^6 Hz at a constant voltage level of 0.5 V and no DC bias.

3.3. Calibration and Compensation. The equipment is calibrated by performing a phase compensation with a 4294A-1D5 high-stability frequency reference (Agilent, Santa Clara, CA), which consists of a 100 Ω resister, and then loading the data measurements into the instrument. A short compensation is also performed using a shorting plate with a 1.3×10^{-3} m spacer in the liquid test fixture to account for lead capacitance. The capacity values are verified with toluene and air. To correct for stray capacitance, all dielectric storage and loss data are multiplied by a correction factor α calculated from[15]

$$\alpha = \frac{100|\varepsilon|}{97.0442|\varepsilon| + 2.9558} \tag{13}$$

To assess the measurement uncertainty, the measurement process is repeated 3 times and the average values of dielectric storage and loss together with the corresponding experimental standard deviations are determined.

4. Results and Discussion

An implementation of the nonlinear least-squares (NLLS) Marquardt−Levenberg algorithm in the Z-view software (Scribner Associates, Southern Pines, NC) is used to fit an electrical model to the experimental data. The equivalent circuit allows for the establishment of correlations between electrochemical system parameters and characteristic impedance elements. The data are successfully modeled as a Randles circuit using Z-view software, in agreement with previous work.[13] The equivalent circuit contains a resistance R_s in series with parallel resistive R_p and capacitive C_p elements as shown in Figure 1. R_s and R_p represent dissipation because of solvent (toluene) and conductive asphaltenes, respectively. C_p represents insulation because of nonconductive asphaltenes (such as dipoles). The capacitance and resistances of the equivalent circuit provided by the fit are independent of frequency. The values of C_p and R_p are in the pF and MΩ range, respectively. On the other hand, R_s is about 2.4 Ω and, thus, is much smaller than R_p.

(15) Agilent 16452A Liquid Test Fixture: Operation and Service Manual. Agilent, Santa Clara, CA, 2000.

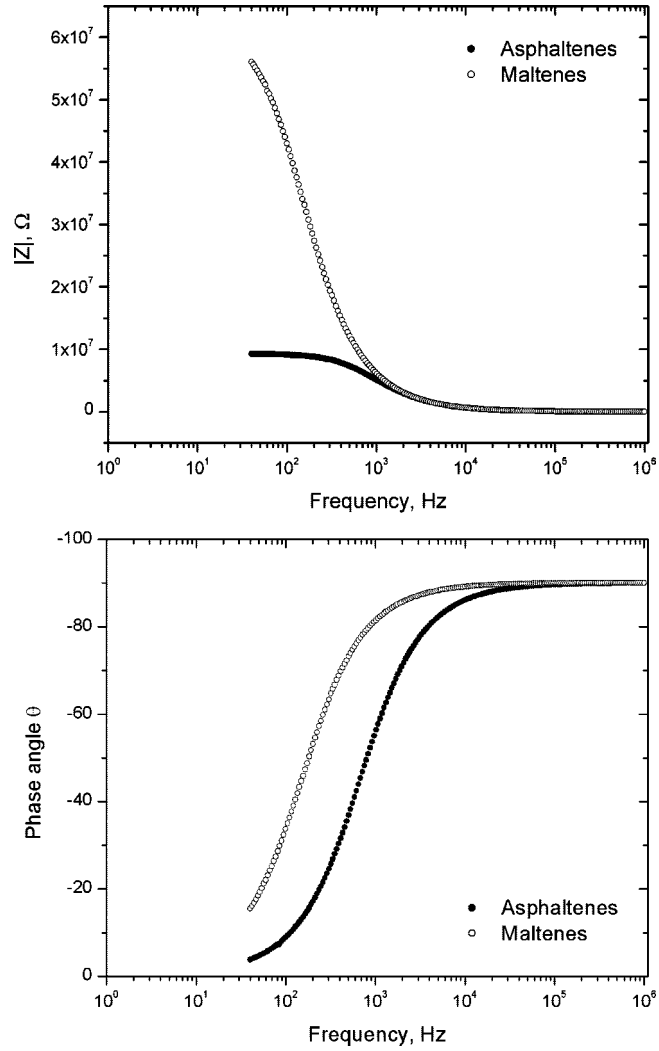

Figure 2. Bode plots of 0.824×10^{-3} kg/L asphaltenes and 3.617×10^{-3} kg/L maltenes in toluene.

The equation describing complex impedance is as follows:

$$Z = \frac{R_p(1 + jR_sC_p\omega)}{1 + jC_p\omega(R_p + R_s)} \tag{14}$$

from which the real part Z' and imaginary part Z'' are

$$Z' = R_\infty + \frac{R_p^{\,2}}{(R_p + R_s)(1 + \omega^2 C_p^{\,2}(R_p + R_s))^2} \tag{15}$$

$$Z'' = \frac{-(R_p - R_\infty)\omega C_p(R_p + R_s)}{1 + \omega^2 C_p^{\,2}(R_p + R_s)^2} \tag{16}$$

where R_∞ is given by

$$R_\infty = \frac{R_pR_s}{R_p + R_s} \tag{17}$$

The DC conductivity is calculated from the electrode/cell geometry and the resistance of the system according to

$$\sigma_{DC} = \frac{t}{A(R_p + R_s)} \tag{18}$$

and the real part of AC conductivity can be determined from

$$\sigma'_{AC} = \frac{t}{A}\frac{R_p + R_s + \omega^2 R_s R_p^{\,2} C_p^{\,2}}{(R_p + R_s)^2 + (\omega R_s R_p C_p)^2} \tag{19}$$

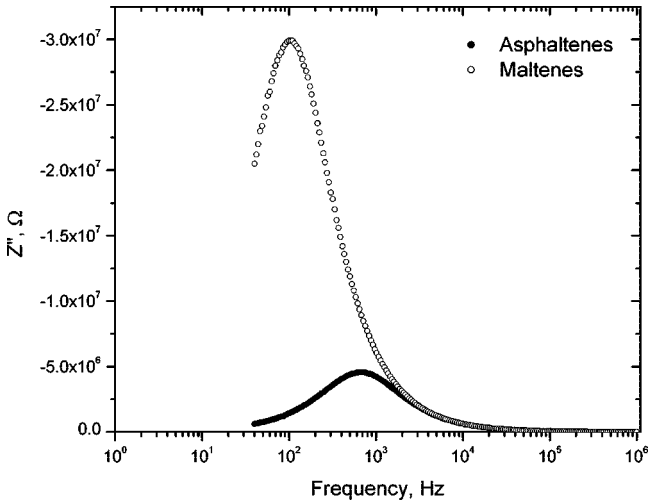

Figure 3. Imaginary part of impedance versus frequency for 0.824 × 10^{-3} kg/L asphaltenes and 3.617 × 10^{-3} kg/L maltenes in toluene.

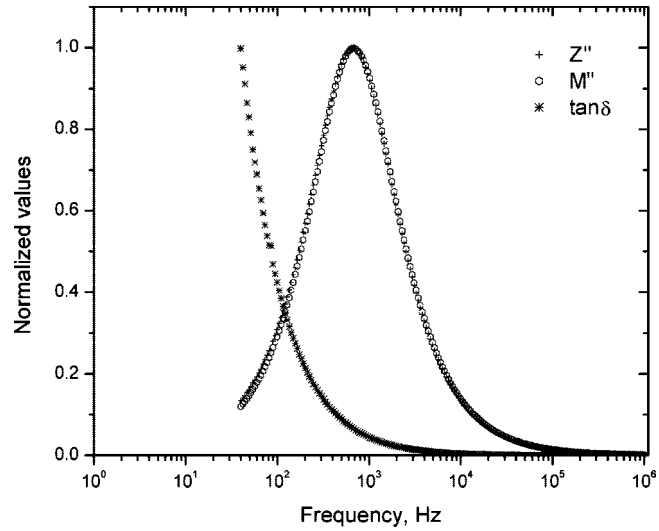

Figure 4. Normalized Z'', M'', and tan δ versus frequency for 0.824 × 10^{-3} kg/L asphaltenes in toluene.

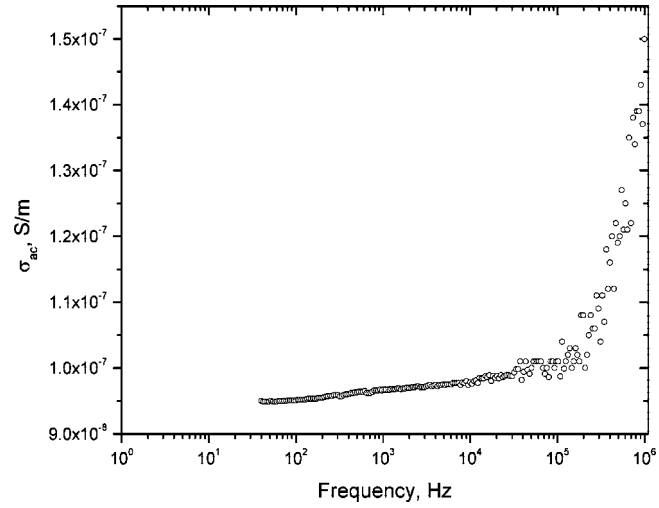

Figure 5. AC conductivity versus frequency for 0.824 × 10^{-3} kg/L asphaltenes in toluene.

The Nyquist plot (also called Argand or Cole−Cole diagram) of 0.824 × 10^{-3} kg/L asphaltenes and 3.617 × 10^{-3} kg/L maltenes in toluene is shown in Figure 1 between 40 and 10^6 Hz. The single semicircle indicates that only one primary relaxation mechanism exists within the frequency range investigated. The right-side intercept of the semicircle with the real axis at low frequency represents the bulk resistance R_p, while the left-side intercept at high frequency represents the solvent resistance R_s. The angle by which the semicircular arc is depressed below the real axis is related to the width of the relaxation time. The absence of a low-frequency tail suggests no electrode polarization effects. The partial semicircle in the case of maltenes indicates a relaxation with relatively small strength. Moreover, the bulk resistance R_p of maltenes is quite large because maltenes contain less conductive species than asphaltenes.

The Bode plots (Figure 2) represent the variations of absolute impedance and phase angle with frequency for asphaltenes and maltenes. As frequency increases, the circuit shifts from highly conducting ($|Z| = R_p$, $\theta \approx 0°$) below ~10 Hz to highly insulating ($|Z| = 0$, $\theta = -90°$) above 10^5 Hz. The transition region between 10 and 10^5 Hz is characterized by an inflection point in Figure 2, which corresponds to the maximum peak in the imaginary impedance versus frequency plot (Figure 3). To better understand the nature of this relaxation, the normalized values of Z'', M'', and tan δ are compared in Figure 4 for 0.824 × 10^{-3} kg/L asphaltenes in toluene. The fact that Z'' and M'' overlap in a frequency region where tan δ is relatively small is a strong indication that conduction is the dominant process.[16] The rapidly increasing value of tan δ at lower frequencies (see Figure 4) is a manifestation of a critical frequency (that is, 10^5 Hz), which represents the start of the transition region in Figure 2. This critical frequency also represents the frequency at which σ'_{AC} reaches almost a plateau value, as shown in Figure 5.

The variations of the real and imaginary components of permittivity with frequency between 40 and 10^6 Hz are presented in Figure 6. The dielectric loss and storage are determined from the impedance data of 0.824 × 10^{-3} kg/L asphaltenes and 3.617 × 10^{-3} kg/L maltenes in toluene with a standard deviation of ~0.01. The observed exponential decrease with frequency could not be described by the Cole−Cole formalism. However, the dielectric loss can be represented by $\sigma_{DC}/\omega\varepsilon_0$ because it is dominated by the DC conductivity.

Figure 7 depicts the effect of the asphaltene concentration on DC conductivity. The conductivity is originally zero because toluene is not conductive. The conductivity then increases with the asphaltene concentration because of the increased ion mobility or reduced activation energy for charge transfer. The onset of asphaltene aggregation can be seen as a clear breakpoint in the variation of conductivity with concentration, in agreement with previous studies.[11] The breakpoint occurs at around 50 × 10^{-6} kg/L (or 50 ppm) asphaltenes in toluene, which is usually known as the onset of dimer formation.[17] This breakpoint could also represent the critical nanoaggregate concentration (CNAC).[18] In the monomer region, the average conductivity is 7 × 10^{-09} S/m and is very similar to values reported by Maruska and co-workers.[6] The DC conductivity is related to the effective diffusion coefficient of asphaltene monomers via the Nernst−Einstein equation

(16) Gerhardt, R. Impedance and dielectric spectroscopy revisited: Distinguishing localized relaxation from long-range conductivity. *J. Phys. Chem. Solids* **1994**, *55* (12), 1491–1506.

(17) Acevedo, S.; Ranaudo, M. A.; Pereira, J. C.; Castillo, J.; Fernàndez, A.; Pérez, P.; Caetano, M. Thermo-optical studies of asphaltene solutions: Evidence for solvent−solute aggregate formation. *Fuel* **1999**, *78*, 997–1003.

(18) Huang, Z.; Song, Y.-Q.; Johnson, D. L.; Mullins, O. C. Critical nanoaggregate concentration of asphaltenes by direct-current (DC) electrical conductivity. *Energy Fuels* **2009**, in press.

$$D = \frac{k_B T \sigma_{DC}}{C_{ion} e^2} \tag{20}$$

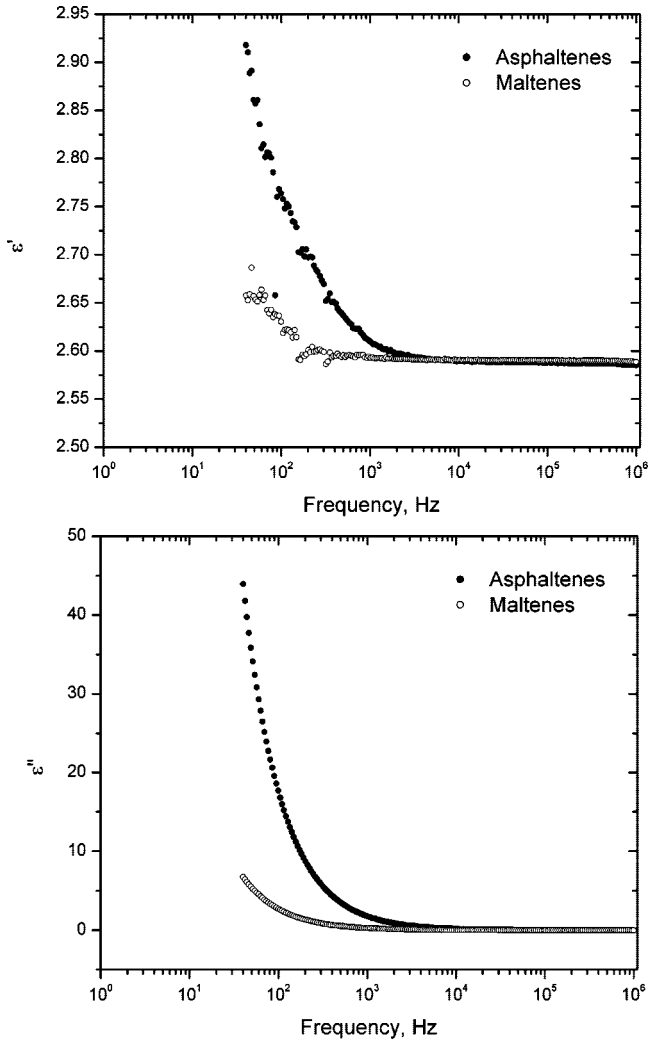

Figure 6. Dielectric storage and loss of 0.824×10^{-3} kg/L asphaltenes and 3.617×10^{-3} kg/L maltenes in toluene.

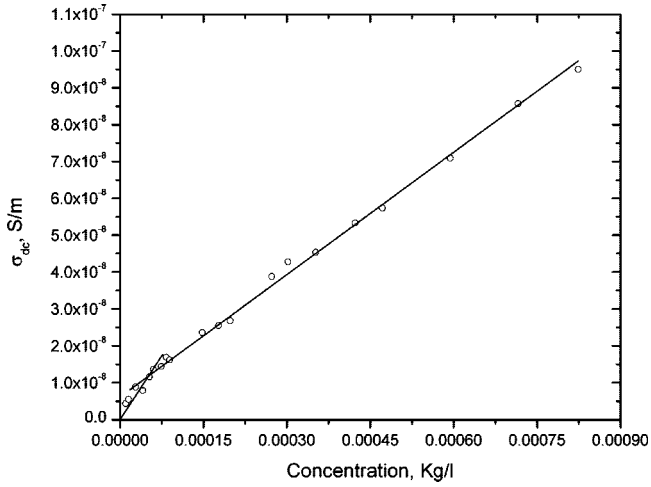

Figure 7. Variations of DC conductivity with asphaltene concentration in toluene. The breakpoint in the curve represents the onset of asphaltene aggregation.

where k_B is the Boltzmann constant ($1.380\,65 \times 10^{-23}$ m^2 kg s^{-2} K^{-1}), T is the absolute temperature, e is the ionic charge ($1.602\,176\,5 \times 10^{-19}$ C), and C_{ion} is the number of diffusing ions per cubic meter of solution given by

$$C_{ion} = \frac{CN_A x}{M} \tag{21}$$

where C is the concentration of asphaltenes in kg/L, N_A is Avogadro's number ($6.022\,141\,8 \times 10^{23}$), M is the molecular weight of asphaltenes (~0.750 kg/mol),[19] and x is the ionic fraction of asphaltenes ($\sim 10^{-5}$).[18]

Assuming particles with a spherical shape; their diameters d are calculated from the Stokes−Einstein equation, where η_s is the viscosity of toluene[20]

$$d = \frac{k_B T}{3\pi \eta_s D} \tag{22}$$

For instance, the diameter of 0.041×10^{-3} kg/L asphaltenes in toluene calculated from the above equations is $\sim 4 \times 10^{-10}$ m (or 4 Å), which is slightly smaller than data found in the literature.[19,21,22]

4. Conclusions

The dielectric relaxation of Boscan asphaltenes and maltenes in toluene is studied in the $40-10^6$ Hz frequency range. The Nyquist and Bode plots indicate that the system is completely conducting below 10 Hz (ideal resistor) and completely insulating above 10^5 Hz (ideal capacitor). The transition region spans from 10 to 10^5 Hz, in which a single relaxation process dominated by conduction effects is measured. Above 10^5 Hz, the AC conductivity increases drastically with frequency. Extrapolation of AC conductivity to zero frequency allows for the estimation of DC conductivity. A breakpoint in the variations of DC conductivity with asphaltene concentration occurs at around 50×10^{-6} kg/L (or 50 ppm) asphaltenes in toluene, which corresponds to the onset of asphaltene aggregation. The average conductivity of asphaltene monomers is 7×10^{-09} S/m, from which the average diameter is $\sim 4 \times 10^{-10}$ m. Thus, the data derived from low-frequency dielectric relaxation are important in predicting asphaltene-associated problems. Low-frequency measurements can also produce sensor responses that are sensitive to interactions between asphaltenes and surfactants usually employed in chemical flooding.

Acknowledgment. The author thanks Dr. Oliver Mullins and Dr. Huang Zeng from Schlumberger for much helpful discussions.

EF800860X

(19) Groenzin, H.; Mullins, O. C. Asphaltene molecular size and structure. *J. Phys. Chem. A* **1999**, *103*, 11257.

(20) Robinson, R. A.; Stokes, R. H. *Electrolyte Solutions, the Measurement and Interpretation of Conductance, Chemical Potential, and Diffusion in Solutions of Simple Electrolytes*; Butterworths Scientific Publications: London, U.K., 1959.

(21) Yen, T. F.; Erdman, J. G.; Pollack, S. S. Investigation of the structure of petroleum asphaltenes by X-ray diffraction. *Anal. Chem.* **1961**, *33* (11), 1587–1594.

(22) Groenzin, H.; Mullins, O. C. Molecular sizes of asphaltenes from different origin. *Energy Fuels* **2000**, *14*, 677.